NJC

Accepted Manuscript

This article can be cited before page numbers have been issued, to do this please use: D. Nematollahi and E. Salahifar, *New J. Chem.*, 2015, DOI: 10.1039/C5NJ00087D.

View Article Online
DOI: 10.1039/C5NJ00087D

NJC

RSCPublishing

PAPER

Electrochemical generation of Michael acceptor: A green method for the synthesis of 4-amino-3-(phenylsulfonyl)diphenylamine derivatives†

Eslam Salahifar and Davood Nematollahi*

Cite this: DOI: 10.1039/xoxxoooooox

Received ooth January 2012,
Accepted ooth January 2012

DOI: 10.1039/xoxxoooooox

www.rsc.org/

Electrochemical oxidation of 4-aminodiphenylamine in aqueous solution and in the presence of some aryl sulfinic acids as nucleophiles was studied and its reaction mechanism was discussed. Using the voltammetric data, a one-pot and environmentally friendly electrochemical approach for the synthesis of 4-amino-3-(phenyl sulfonyl)diphenylamine derivatives via the Michael type addition reaction of anodically generated *N*-phenylquinone diimine with aryl sulfinic acids, at a carbon electrode, without toxic reagents and solvents is reported.

Introduction

Arylsulfone compounds are widely used as building blocks for some drugs, such as Laropiprant and Vioxx. They have also been shown to have antibacterial, antifungal and antitumor properties.[1,2] On the other hand, diphenylsulfone compounds were found to exhibit anti-bacterial activity.[3] The incorporation of a diphenylsulfone moiety into some heterocyclic compounds was found to increase their biological activity.[4] For example, diphenylsulfone is used for the synthesis of dapsone (4,4-diaminodiphenylsulfone) (Figure 1) which is a bacteriostatic drug that inhibits dihydrofolic acid synthesis by competition with *para*-aminobenzoic acid.[5] It was also shown that, dapsone has anti-inflammatory and bacteriostatic properties comparable with those of nonsteroidal anti-inflammatory drugs.[6,7] In addition, it can inhibit cellular adhesion, chemotaxis, and the expression of prostaglandin, leukotrienes, IL-8, TNFα.[8]

The most common methods for the synthesis of sulfone derivatives are the sulfonylation of arenes using aryl sulfonyl halides, the oxidation of sulfides or aryl sulfonic acids in the presence of a strong acid catalyst.[9-11] Major disadvantage of these methods is an incompatibility with numerous functional groups.[12] Our interest in the design and electrochemical synthesis of new compounds with medicinal activity[13-16] prompted us to synthesize new molecules similar to dapsone under mild and ambient condition. Herein we investigated the electrochemical oxidation of 4-aminodiphenylamine (**4-APA**) in the presence of sulfinic acid sodium salts as nucleophiles and showed that the anodically generated *N*-phenylquinonediimine as a Michael acceptor reacts with sulfinic acids. In this work, we have discovered an easy and one-pot electrochemical method for the synthesis of new 4-amino-3-(phenylsulfonyl) diphenylamine derivatives in the high yield and purity, using an environmentally friendly method with high atom economy. Atom economy is defined as the percentage of reactants that go into final products. From green chemistry and waste management viewpoints, this method also minimizes metallic catalyst consumption as a great pollutant and on the other hand, catalyst recycling cost decreases particularly.[17]

Fig. 1. The structure of dapsone (A) and compounds reported here (B).

Results and discussion

pH studies

Cyclic voltammetry of **4-APA** in aqueous perchloric acid solution (pH = 1.0, c = 0.2 M) is shown in Figure 2, curve d. The voltammogram showed one anodic peak (A_1) at 0.42 V due to the oxidation of **4-APA** to *N*-phenylquinonediimine (***N*-PQD**) and one cathodic peak (C_1) at 0.38 V during the revers scan due to the reduction of ***N*-PQD** to **4-APA** (Scheme 1). Under these conditions, the peak current ratio (I_{pC1}/I_{pA1}) is independent of scan rate and equal to unity which can be considered as a criterion for the stability of electrogenerated ***N*-PQD** under the experimental conditions. In other words, any side reactions, such as hydroxylation,[18] dimerization,[19,20]

oxidative ring cleavage[21] or hydrolysis[22,23] on electrochemically generated ***N*-PQD** are too slow to be observed at the time scale of cyclic voltammetry.

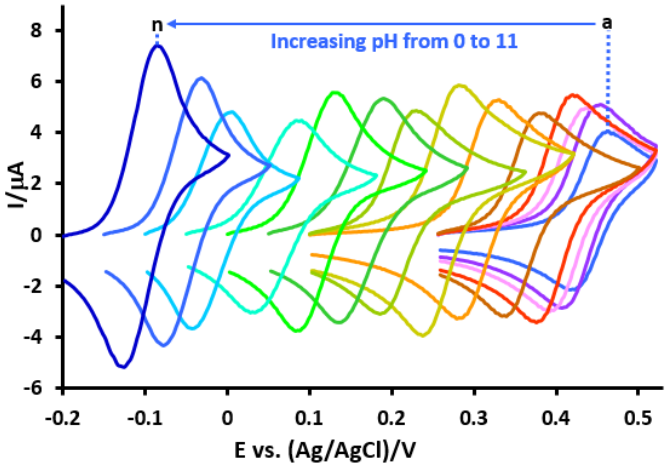

Figure 2. Cyclic voltammograms of **4-APA** (0.5 mM) in aqueous buffer solutions with different pH values and same ionic strength, at a glassy carbon electrode. The pH values from (a) to (n) are: 0.0, 0.2, 0.5, 1.0, 2.0, 3.0, 4.0, 5.0, 6.0, 7.0, 8.0, 9.0, 10.0 and 11.0, respectively. Scan rate; 50 mV s^{-1}. Temperature = 25 ± 1 ºC.

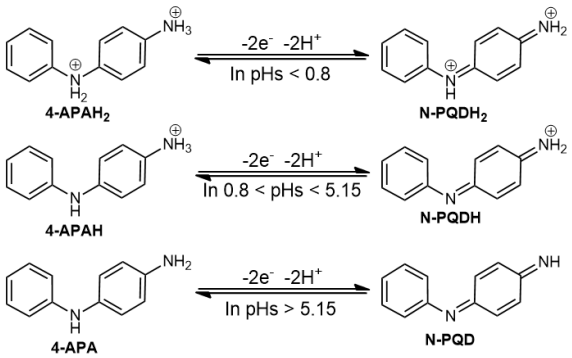

Scheme 1. Electrochemical oxidation of **4-APA** in the pH range 0-11.

It is well known that in the majority of electro-oxidations of organic compounds, the transfer of electron(s) is accompanied by a proton transfer. Therefore, the effects of pH on the electrochemical oxidation of **4-APA** has been studied. Figure 2 also, shows the cyclic voltammograms of **4-APA** in various pHs in the range of 0-11. It was found that the change of pH does not significantly affect the peak current ratio (I_{pC1}/I_{pA1}), while, the half wave potential ($E_{1/2}$) shifted to the negative potentials by increasing pH. The latter is expected because of the participation of proton(s) in the oxidation of **4-APA** to ***N*-PQD**. The half wave potential ($E_{1/2}$), is given by:

$$E'_{1/2} = E_{1/2} - (2.303\ mRT/2F)\ \text{pH}$$

where m is the number of protons involved in the reaction and $E_{1/2}$ is the half wave potential at pH = 0.0, R, T and F have their usual meanings. The half-wave potentials ($E_{1/2}$) were calculated as the average of anodic and cathodic peak potentials of the cyclic voltammograms {(E_{pA1} + E_{pC1})/2}. The values of $E_{1/2}$ as a function of solution's pH are plotted in Fig. 3. As can be seen, $E_{1/2}$ was shifted to negative potentials with the slope of about 50 mV/pH ($E'_{1/2}$ = -0.050pH + 0.45) which is in agreement with the theoretical slope (2.303mRT/2F) of 59 mV/pH with m about 2. This shows that the same numbers of electrons and protons[23,24] are involved in the redox processes, at pH value between 0-11. On the basis of the reported pK_a values of primary and secondary amine moieties of **4-APA** (5.15 and ≈ 0.8, respectively) (Scheme 2),[24] we can conclude Scheme 1 for the electrochemical oxidation of **4-APA** in the pH range 0-11.

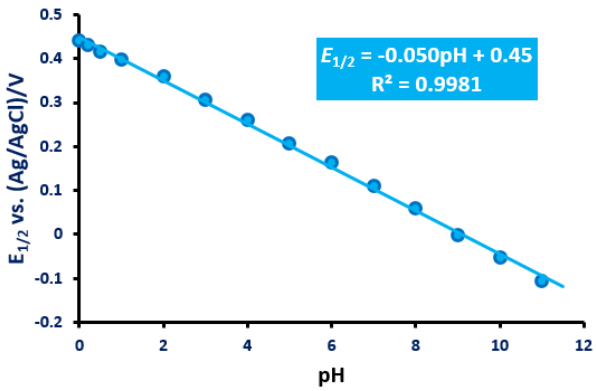

Figure 3. The potential-pH diagram of **4-APA**.

The presence of the same numbers of electrons and protons in the redox processes in pHs less than 5.15 (Scheme 1), shows that the oxidation products are in protonated forms.[24] In pH values less than 0.8, the high acidity of solution may be responsible for the generation of diprotonated quinoid form (**N-DPQH$_2$**) during the oxidation of **4-APA**. Bergamini et al reported that pK_a of **N-DPQH** is about 5.6 (very close to the pK_{a2} for **4-APA**).[24] So, we can assert therefore that the similarity of the basicity of **4-APA** and **N-PQD** can be responsible for the two-electron/two-proton process in 0.8 < pHs < 5.15.

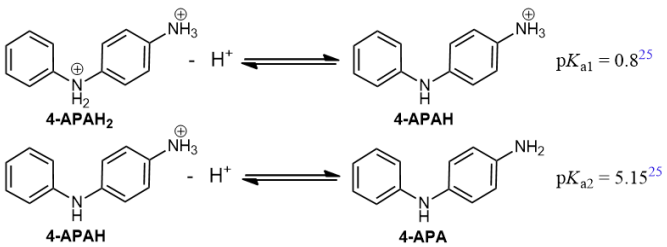

Scheme 2. Acid/base equilibrium of **4-APA**.

Mechanistic studies

The electrochemical oxidation of **4-APA** in the presence of 4-toluenesulfinic acid (**1a**) was also studied in the pH range 2-9 (Figure 4, curves b). A comparison of voltammogram of **4-APA** in the absence of **1a** with that in the absence of **1a** at pH, 2.0 shows that: (a) a new redox couple (A_2/C_2) appears at more positive potentials; (b) the anodic peak A_1 current (I_{pA1})

View Article Online
DOI: 10.1039/C5NJ00087D
Paper

increases slightly and its potential shifts to less positive values and (c) in the reverse scan, the cathodic peak C_1 nearly disappears. These observations indicate that a chemical reaction follows the electron transfer process: ***N*-PQD** formed at the surface of the electrode by the two-electron oxidation of **4-APA** is consumed in a reaction with **1a**. In this Fig. curve c, is cyclic voltammogram of **1a**.

This is further confirmed by the effect of the scan rate and of the concentration of **1a** on the cyclic voltammogram of **4-APA** in the presence of **1a**. Our data shows that, I_{pA1} increases with respect of that of peak A_2 upon increasing the scan rate as does the current of peak C_1 (I_{pC1}) (Figure 5). Such increase at faster scan rates is related to a decrease of the experimental time scale. A faster scan rate results in a lesser amount of ***N*-PQD** reacting with **1a**, hence the observe increase of the peak current ratio (I_{pC1}/I_{pA1}). Figure 5 also shows that E_{pA1} shifts to positive potentials with increasing potential scan rate. Because of the following reaction, E_{pA1} is less positive than E_{pA1} in the absence of **1a** (Fig. 4). However, it shifts in a positive direction (toward the unperturbed curve) with increasing *v* (Figure 5).

In addition, upon the increasing of the concentration of **1a**, I_{pA2} and I_{pC2} increase, and I_{pC1} decreases. Peak A_2 is due to the oxidation of adduct formed by the reaction of ***N*-PQD** with **1a**. The higher the concentration of **1a**, the faster is its reaction with ***N*-PQD**, the lesser is the amount of ***N*-PQD** be reduced (peak C_1).

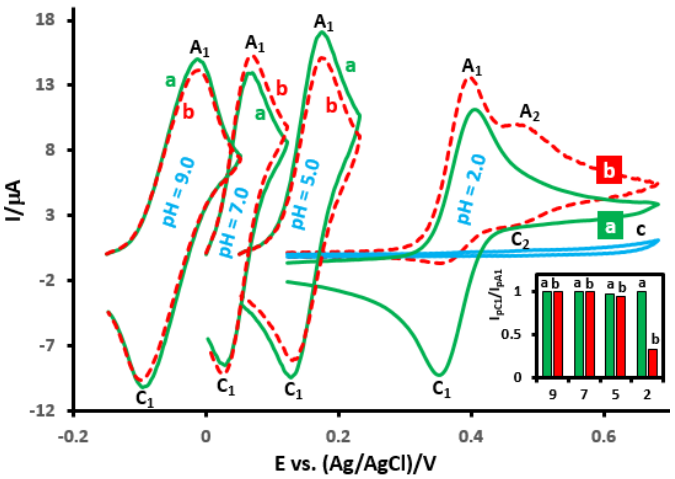

Figure 4. Cyclic voltammograms of 4-**APA** (1.0 mM) (a) in the absence, (b) in the presence of **1a** (1.0 mM). (c) **1a** (1.0 mM) in the absence of **4-APA** at glassy carbon electrode in aqueous buffer solutions with different pH values and same ionic strength. Scan rate; 100 mV s^{-1}. Temperature = 25 ± 1 °C. Inset: A plot of peak current ratio (I_{pA1}/I_{pC1}) in the absence (a) and presence of **1a** (b) in pH values. The pH values are shown on horizontal axis.

Contrary to pH 2.0, the cyclic voltammograms of **4-APA** in the presence of **1a** (curves b) in pH values 5.0, 7.0 and 9.0, do not show any sign of reactivity of ***N*-PQD** toward **1a** in the time scale of our experiments. A plot of peak current ratio (I_{pA1}/I_{pC1}) in the absence (curves a) and presence of **1a** (curves b) in pH values 2-9 is shown in Fig. 4, inset. It was found that the change of pH has only a great influence on the peak current ratio (I_{pC1}/I_{pA1}) in the presence of **1a** in pH 2.0. Since, in cyclic voltammetry, the peak current ratio is a measure of homogeneous reaction rate or reactivity of ***N*-PQD** formed at the surface of the electrode with **1a**,[25] in this study, a solution with pH 2.0 has been selected as a suitable medium for the electrochemical synthesis.

Controlled-potential coulometry was performed in an aqueous phosphate buffer (pH = 2.0, *c* = 0.2 M) solution containing **4-APA** (0.25 mmol) and **1a** (0.25 mmol) at 0.30 V vs. Ag/AgCl. The electrolysis progress was monitored using cyclic voltammetry (Figure 6). As shown, the following changes: a) decrease in the anodic peak current A_1, b) increase in the anodic peak current A_2 and c) disappearance of peak A_1 after consumption of about $2e^-$ per molecule of **4-APA**, are observed in cyclic voltammograms during the advancement of coulometry.

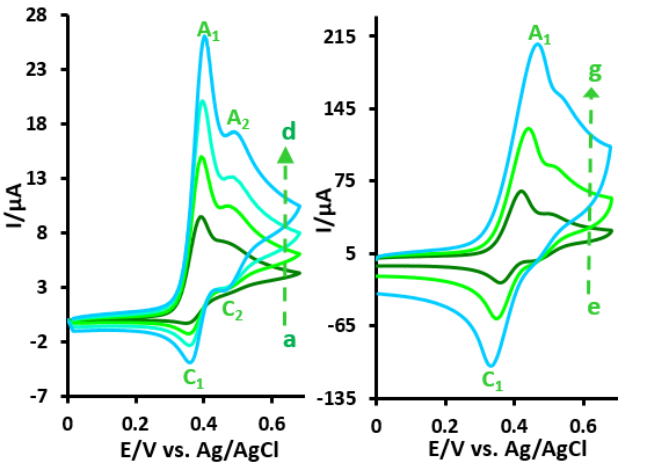

Figure 5. Cyclic voltammograms of **4-APA** (1.0 mM) in the presence of 4-toluenesulfinic acid (**1a**) (1.0 mM) at various scan rates. Scan rates from a) to g) are: 50, 100, 150, 250, 1000, 2500 and 5000 mV s^{-1}, respectively, at glassy carbon electrode in aqueous phosphate buffer (pH = 2.0, *c* = 0.2 M). Temperature = 25 ± 1 °C.

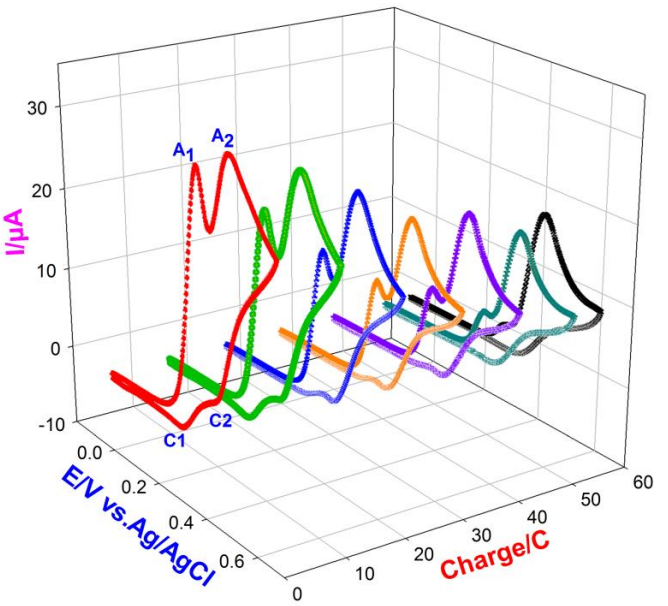

Figure 6. Cyclic voltammograms of 4-**APA** (0.25 mmol) in the presence of 4-toluenesulfinic acid (**1a**) (0.25 mmol) during controlled potential coulometry at 0.30 V *vs*. Ag/AgCl (3 M) in aqueous phosphate buffer (pH = 2.0, *c* = 0.2 M). Scan rate: 100 mV s^{-1}. Temperature =25 ± 1 °C.

The coulometry and voltammetry results, the (^{1}H, ^{13}C) NMR and FTIR data and the molecular mass of 338 of the isolated electrolysis product all point out to N^1-phenyl-3-tosylbenzene-1,4-diamine (**3a**) which would have been formed according to the pathway shown in Scheme 3 (E_rC_i mechanism). In proposed mechanism, for simplification the protonation of species are omitted. The first step (E_r) is the generation of ***N*-PQD**. In the next step, ***N*-PQD** would serve as a Michael acceptor in a reaction with **1a** to form the final product **3a** (C_i step). The oxidation of **3a** is more difficult than the oxidation of **4-APA** due to the presence of the electron-withdrawing tolylsulfonyl group. Therefore, the oxidation of **3a** did not occur during the electrochemical oxidation at the potential of 0.30 V. According to the proposed mechanism, the anodic peak A_2 should correspond to the oxidation of **3a** to the quinonediimine $\mathbf{3a_{ox}}$. Obviously, the cathodic peak C_2 corresponds to the reduction of $\mathbf{3a_{ox}}$ to **3a**.

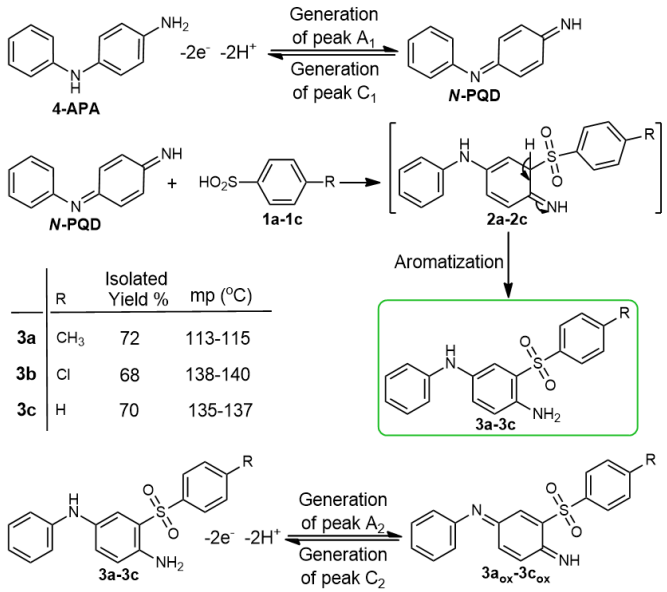

	R	Isolated Yield %	mp (°C)
3a	CH_3	72	113-115
3b	Cl	68	138-140
3c	H	70	135-137

Scheme 3. Electrochemical oxidation of **4-APA** in the presence of **1a-1c.**

Figure 7 shows the variation of anodic peak current (I_{pA1}) versus consumed charge (all data obtained from Fig. 6). As expected, a linear relationship was found between I_{pA1} and the consumed charge. The equation of the line is I_{pA1} = -0.49Q + 28.8, with a correlation coefficient, R= 0.995. Using these data, the current efficiency for the electrochemical synthesis of **3a** was calculated based on Faraday's law (deviation between theoretical and experimental charge). The calculated current efficiency value is about 82%. The same data were obtained for the electrochemical synthesis of **3b** and **3c**.

To calculate atom economy, equation (1) was used, according to Eissen and coworkers.[26]

$$\% \text{ Atom Economy} = \frac{\text{Mass of atoms in desired product}}{\text{Mass of atoms in reactants}} \times 100 \quad \text{Eq. 1}$$

According to Scheme 3, the overall reaction mechanism for electrochemical synthesis of **3a-3c** is shown in Scheme 4:

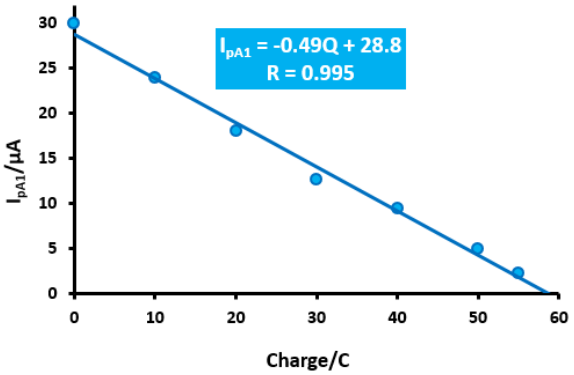

Figure 7. Variation of anodic peak current (I_{pA1}) versus consumed charge. All data obtained from Fig. 6.

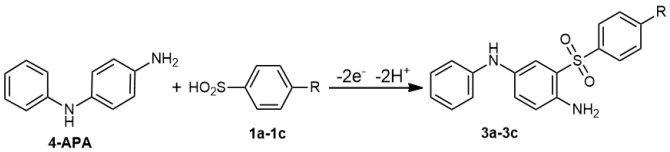

Scheme 4. The overall reaction of electrooxidation of **4-APA** in the presence of **1a-1c.**

The calculated atom economy for the synthesis **3a-3c** are 99.41, 99.39 and 99.45%, respectively. The high atom economy indicates that all atoms (except two hydrogen atoms) from the two starting materials are incorporated into the product.

***N*-PQD** can be attacked by **1c** from sites A or B to yield two types of compounds (**3c** and **4c**) (Scheme 5). However, single-crystal X-ray diffraction analysis of synthesized compound confirms the structure of **3c** (Figure 8).

This regioselectivity may presumably be due to the large steric hindrance in the molecule **4c** in comparison with **3c**. The steric energies have been calculated for **3c** and **4c**, using MM2 program after minimization of structures (Fig. 9). Results indicate that structure **3c** is energetically more stable than the **4c** with about 11 kcal/mol lower energy.

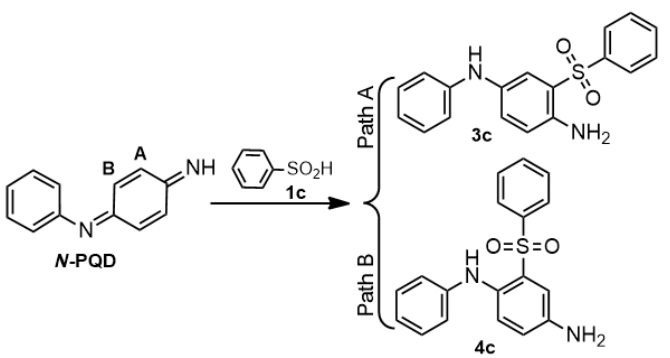

View Article Online
DOI: 10.1039/C5NJ00087D
Paper

Scheme 5. The structures of possible compounds.

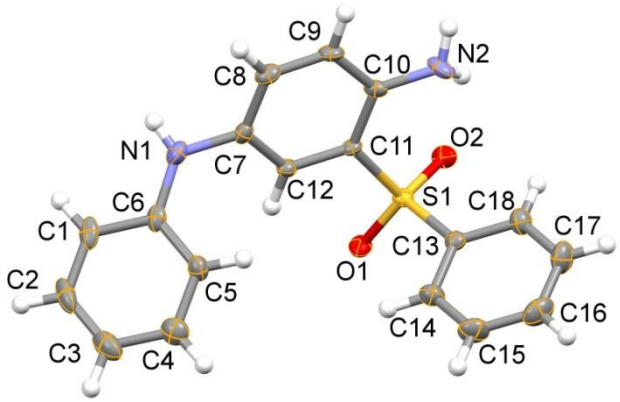

Figure 8. ORTEP view of X-ray crystal structure of **3c**.

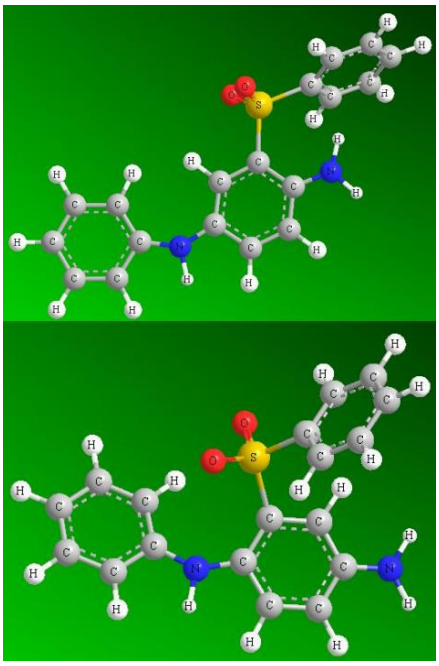

Figure 9. The results of MM2 calculation for **3c** (above) and **4c** (below).

In order to investigate the electrochemical properties of the isolated product (**3c**), its voltammetric behavior was examined. The cyclic voltammogram of saturated solution of **3c** in aqueous phosphate buffer (pH = 2.0, *c* = 0.2 M)/ethanol (90/10 v/v) is shown in Fig. 10. Contrary to **4-APA**, in potential scan rate 100 mV s^{-1}, it shows an irreversible feature with one anodic peak (A_2) at 0.44 V vs. SCE which corresponds to the transformation of **3c** to $\mathbf{3c_{ox}}$ (Scheme 3). In addition, in comparison with **4-APA**, E_{pA2} is more positive than E_{pA1}. The results were predictable. In general, the attachment of an electron-withdrawing group (*EWG*) to a molecule, unstable the oxidized form of molecule and arrives it in the fast following chemical reaction(s).[13,27] In this case, the presence of arylsulfonyl group with electron withdrawing character in the structure of **3c** unstable the electro-generated quinonediimine $\mathbf{3c_{ox}}$ and arrives it in the fast following chemical reactions such as hydroxylation,[18] dimerization,[19,20] oxidative ring cleavage[21] and/or hydrolysis.[22,23]

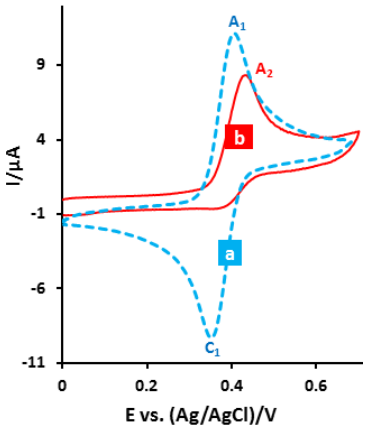

Figure 10. (a) Cyclic voltammogram of **4-APA** (1.0 mM) and (b) cyclic voltammogram of saturated solution of **3c** at glassy carbon electrode in aqueous phosphate buffer (pH = 2.0, *c* = 0.2 M)/ethanol (90/10 v/v) mixture. Scan rate; 100 mV s^{-1}. Temperature = 25 ± 1 °C.

The effect of the potential scan rate on the cyclic voltammogram of **3c** was also studied (Fig. 11). The obtained data show that with increasing scan rate, the peak current ratio (I_{pC2}/I_{pA2}) increase. The time scale of a cyclic voltammetry experiment is determined by the potential scan rate, as increasing the scan rate decreases the experimental time scale and removes the effects of the following chemical reaction(s) appearing as an increase in I_{pC2}/I_{pA2}.

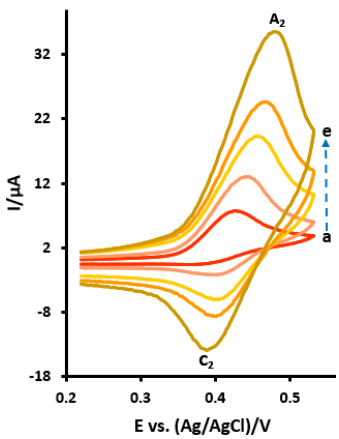

Figure 11. Cyclic voltammograms of saturated solution of **3c** at glassy carbon electrode in aqueous phosphate buffer (pH = 2.0, *c* = 0.2 M)/ethanol (90/10 v/v) mixture in different scan rate. Scan rates from a to e are: 100, 250. 500, 750 and 1000 mV s^{-1}. Temperature = 25 ± 1 °C.

Conclusions

The present method for the synthesis of 4-amino-3-(phenylsulfonyl)diphenylamine derivatives has several advantages over conventional methods. This process is practically convenient to carry out and can be performed at atmospheric pressure and room temperature. Neither catalyst nor organic/inorganic oxidizing agents are necessary and the

reaction can be performed under green and mild condition with high atom economy (>99%). The in situ formation of *N*-phenylquinonediimine is achieved and there is no need to prepare *N*-phenylquinonediimine in advance.

Experimental section

Apparatus and reagents

The working electrode used in macro-scale electrolysis and controlled-potential coulometry was an assembly of four ordinary soft carbon rods (6 mm diameter and 4 cm length), placed as single rods in the edges of a square with a distance of 3 cm, and a large stainless steel cylinder (25 cm^2 area) constituted the counter electrode. The working electrode used in the cyclic voltammetry experiments was a glassy carbon disc (1.8 mm diameter) and a glass carbon rod was used as the counter electrode. The electrosynthesis were performed under controlled-potential condition in a two compartments cell, separated by an ordinary porous fritted-glass diaphragm (a tube with 1.5 cm diameter) and equipped with a magnetic stirrer. **4-APA**, aryl sulfinic acids, phosphate salts and ethanol were obtained from commercial sources. These chemicals were used without further purification. The glassy carbon electrode was polished using alumina slurry (from Iran Alumina Co.). More details are described in the previous paper.[28]

Electroorganic synthesis of 3a-3c.

A solution of phosphate buffer (c = 0.2 M, pH = 2.0)/ethanol (50/50 v/v) mixture, containing **4-APA** (0.25 mmol) and **1a** (**1b** or **1c**) (0.25 mmol), was electrolyzed in a divided cell at 0.30 V vs. Ag/AgCl (3M). The electrolysis was terminated when the decay of current became more than 95%. At the end of electrolysis, the cell was placed in a refrigerator overnight. The precipitated solid was collected by filtration and recrystallized from acetone/*n*-hexane mixture (30/70 v/v).

N^1-Phenyl-3-tosylbenzene-1,4-diamine ($C_{19}H_{18}N_2O_2S$) (3a)

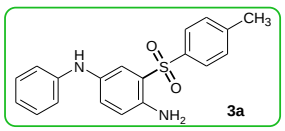

Isolated yield: 72%. IR (KBr, cm^{-1}): 3429, 3347, 1599, 1514, 1284, 1142, 751, 586. ^{1}H NMR (400 MHz DMSO-d_6): δ 2.36 (s, 3H, methyl), 5.83 (s, 2H, NH_2, disappeared by the addition of D_2O), 6.71 (t, 1H), 6.76 (d, 2H, J = 8.8 Hz), 6.83 (d, 2H, J = 7.6 Hz), 7.12-7.18 (m, 3H), 7.40 (d, 2H, J = 8.4 Hz), 7.44 (d,1H, J = 2.4 Hz), 7.81 (d, 2H, J = 8.4 Hz), 7.86 (s, 1H, NH, disappeared by the addition of D_2O). ^{13}C NMR (100 MHz DMSO-d_6): δ 21.5, 115.0, 118.8, 119.0, 119.1, 120.8, 127.2, 128.6, 129.7, 130.3, 132.7, 133.8, 142.3, 144.4, 145.5. MS (EI) *m/z* (relative intensity): 338 (100), 263 (41), 236 (38), 183 (41), 154 (29), 69 (38).

3-((4-Chlorophenyl)sulfonyl)-N^1-phenylbenzene-1,4-diamine ($C_{18}H_{15}ClN_2O_2S$) (3b)

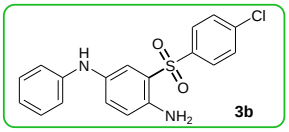

Isolated yield: 70%. IR (KBr, cm^{-1}): 3428, 3353, 2923, 2853, 1631, 1598, 1516, 1486, 1397, 1314, 1146, 1088, 758, 587, 480. ^{1}H NMR (400 MHz DMSO-d_6): δ 5.86 (s, 2H, NH_2, disappeared by the addition of D_2O), 6.72 (t, 1H), 6.79 (d, 2H, J = 8.8 Hz), 6.84 (d, 2H, J = 8.0 Hz), 7.17 (m, 3H), 7.44 (d, 1H, J = 2.4 Hz), 7.68 (dd, 2H, J = 8.8, 2.0 Hz) 7.89 (s, 1H, NH, disappeared by the addition of D_2O), 7.94 (dd, 2H, J = 8.8, 2.0 Hz). ^{13}C NMR (100 MHz DMSO-d_6): δ 115.1, 118.7, 118.9, 119.3, 119.9, 128.9, 129.1, 129.7, 130.0, 132.9, 138.9, 140.4, 142.5, 145.4. MS (EI) *m/z* (relative intensity): 358 (21), 324 (14), 252 (100), 195 (43), 171 (64), 135 (75), 85 (86).

N^1-phenyl-3-(phenylsulfonyl)benzene-1,4-diamine ($C_{18}H_{16}N_2O_2S$) (3c)

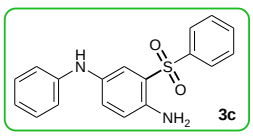

Isolated yield: 72%. IR (KBr, cm^{-1}): 3451, 3404, 3366, 1634, 1598, 1505, 1312, 1292, 1142, 1095, 751, 588, 537. ^{1}H NMR (400 MHz DMSO-d_6): δ 5.86 (s, 2H, NH_2, disappeared by the addition of D_2O), 6.72 (t, 1H), 6.78 (d, 1H, J = 8.8 Hz), 6.83 (d, 2H, J = 7.6 Hz), 7.15 (m, 3H), 7.45 (d, 1H, J = 2.4 Hz), 7.61 (t, 2H), 7.69 (t, 1H), 7.88 (s, 1H, NH, disappeared by the addition of D_2O), 7.93 (dd, 2H, J = 8.4, 1.6 Hz). ^{13}C NMR (100 MHz DMSO-d_6): δ 115.0, 118.8, 119.0, 119.1, 120.4, 127.1, 128.7, 129.7, 129.9, 132.8, 133.9, 141.7, 142.5, 145.5. MS (EI) *m/z* (relative intensity): 324 (39), 252 (55), 223 (17), 195 (38), 149 (28), 115 (61), 55(100).

Acknowledgements

We acknowledge the Bu-Ali Sina University Research Council and the Center of Excellence in Development of Environmentally Friendly Methods for Chemical Synthesis (CEDEFMCS) for their support of this work.

Notes and references

Faculty of Chemistry, Bu-Ali-Sina University, Hamedan 65178-38683, I. R. Iran. nemat@basu.ac.ir

† Electronic Supplementary Information (ESI) available: FT-IR, ^{1}H NMR and ^{13}C NMR spectra of **3a-3c** and crystallographic Information data of **3c** (CIF). See DOI: 10.1039/c000000x/

1 Z. Y. Sun, E. Botros, A. D. Su, Y. Kim, E. Wang, N. Z. Baturay and C. H. Kwon, *J. Med. Chem.*, 2000, **43**, 4160-4168.

2 T. Otzen, E. G. Wempe, B. Kunz, R. Bartels, G. Lehwark-Yvetot, W. Hänsel, K. J. Schaper and J. K. Seydel, *J. Med. Chem.*, 2003, **47**, 240-253.

3 E. F. Elslager, Z. B. Gavrilis, A. A. Phillips and D. F. Worth, *J. Med. Chem.*, 1969, **12**, 357–363.

View Article Online
DOI: 10.1039/C5NJ00087D
Paper

4 G. L. Almajan, S. F. Barbuceanu, E. R. Almajan, C. Draghici and G. Saramet, *Eur. J. Med. Chem.*, 2009, **44**, 3083–3089.
5 M. D. Coleman, *Br. J. Dermatol.*, 1993, **129**, 507-513.
6 S. Repichet, C. Le Roux, P. Hernandez and J. Dubacjean-Roger, *J. Org. Chem.*, 1999, **64**, 6479–6482.
7 M. D. Coleman and M. D. Tingle, *Drug Dev. Res.*, 1992, **25**, 1–16.
8 G. Wozel and C. Blasum, *Arch. Dermatol. Res.*, 2014, **306**, 103-124.
9 K. Schank, In *The Chemistry of Sulfones and Sulfoxides*: S. Patai, Z. Rappopor and C. J. M. Stirling, Eds.; Wiley: New York, 1988; Chapter 7.
10 W. E. Truce, T. C. Klinger and W. W. Brand, In *Organic Chemistry of Sulfur:* S. Oae, Ed.; Plenum Press: New York, 1977.
11 H. Suzuki and H. Abe, *Tetrahedron Lett.*, 1995, **36**, 6239-6242.
12 J. M. Baskin and Z. Wang, *Org. Lett.*, 2002, **4**, 4423-4425.
13 F. Varmaghani, D. Nematollahi, S. Mallakpour and R. Esmaili, *Green Chem*., 2012, **14**, 963-967.
14 D. Nematollahi and M. Rafiee, *Green Chem.*, 2005, **7**, 638–644.
15 H. Salehzadeh, D. Nematollahi and H. Hesari, *Green Chem*., 2013, **15**, 2441-2446.
16 A. Maleki and D. Nematollahi, *Org. Lett.*, 2011, **13**, 1928–1931.
17 B. A. Frontana-Uribe, R. D. Little, J. G. Ibanez, A. Palmad and R. Vasquez-Medrano, *Green Chem.*, 2010, **12**, 2099–2119.
18 L. Papouchado, G. Petrie, J. H. Sharp amd R. N. Adams, *J. Am. Chem. Soc*., 1968, **90**, 5620-5621.
19 H. Salehzadeh, D. Nematollahi and M. Rafiee, *J. Electroanal. Chem.*, 2011, **650**, 226-232.
20 D. Nematollahi, M. Rafiee and A. Samadi-Maybodi, *Electrochim. Acta*, 2004, **49**, 2495-2502.
21 D. Nematollahi and F. Varmaghani, *J. Iran. Chem. Soc*., 2011, **8**, 803-810.
22 H. Yang and A. J. Bard, *J. Electroanal. Chem.*, 1992, **339**, 423-449.
23 R. L. Hand and R. F. Nelson, *J. Am. Chem. Soc.*, 1974, **96**, 850-860.
24 J. F. Bergamini, M. Belabbas, M. Jouini, S. Aeiyach, J. C. Lacroix, K. I. Chane-Ching and P. C. Lacaze, *J. Electroanal. Chem*., 2000, **482**, 156-67.
25 A. J. Bard and L. R. Faulker, *Electrochemical Methods*, 2nd ed., Wiley, New York, 2001.
26 M. Eissen, R. Mazur, H. G. Quebbemann and K. H. Pennemann, *Helv. Chim. Acta*, 2004, **87**, 524–535.
27 D. Nematollahi, A. Sayadi and F. Varmaghani, *J. Electroanal. Chem.*, 2012, **671**, 44−50.
28 D. Nematollahi, S. Dehdashtian and A. Niazi, *J. Electroanal. Chem.*, 2008, **616**, 79-86.